Optical detection and imaging of nonequilibrium phonons in GaAs using excitonic photoluminescence

M. T. Ramsbey*
Physics Department and Materials Research Laboratory, University of Illinois at Urbana-Champaign, Urbana, Illinois 61801

I. Szafranek and G. Stillman
Department of Electrical and Computer Engineering and Materials Research Laboratory, University of Illinois at Urbana-Champaign, Urbana, Illinois 61801

J. P. Wolfe
Physics Department and Materials Research Laboratory, University of Illinois at Urbana-Champaign, Urbana, Illinois 61801
(Received 8 November 1993)

We have developed a time- and space-resolved optical detector of nonequilibrium phonons utilizing excitonic photoluminescence at low temperatures. An epilayer of GaAs is "sensitized" by excitation with a low-power, focused "probe" beam, which creates free excitons (FE's) and bound excitons (BE's) in the layer. The photoluminescence intensity from these species is reduced by a flux of nonequilibrium phonons, created on the opposite side of the GaAs substrate by optical excitation of a metal film with a "pump" beam. A simple model is proposed for the phonon-induced change in photoluminescence intensity of the FE's; previous work (e.g., by Blank *et al.* [Sov. Phys. Semicond. **25**, 39 (1991)]) has treated the case of BE's. Both time-resolved heat pulses and space-resolved heat flux associated with phonon focusing are observed. The heat pulses are characterized by a broad temporal distribution, the exact origin of which is not determined. If the sensitivity of this detection technique could be raised sufficiently, space and time resolutions of 1 μm and 1 ns, respectively, would be feasible.

I. INTRODUCTION

Great advances have been made in recent years in the growth of epitaxial crystal layers. Semiconductor layers, grown with a minimum of impurities and crystal defects, exhibit extremely high electron mobilities which exceed those of bulk materials. Such materials have obvious applications in high-speed electronic and optoelectronic devices. Superlattice and quantum-well growth technology allows scientists to tailor material properties and create quantum systems that do not exist in nature. Continual progress in this field requires increased understanding of the composition and behavior of residual defects and their influence on the electrical and optical properties of the epilayer.

In this paper we examine the effects of nonequilibrium acoustic phonons on excitonic states in GaAs at low temperatures. A free exciton (FE) is an electron-hole pair bound by Coulomb forces and produced by photoexcitation of the semiconductor. It is most easily detected by the luminescence accompanying its recombination. Once produced, the exciton can become trapped on shallow impurity sites, giving rise to bound-exciton (BE) luminescence lines shifted in energy from the free-exciton luminescence line. We are interested in how the populations of FE's and BE's are affected by heat pulses introduced in the crystal and, particularly, in the possibility of using the photoluminescence from FE's and BE's as a time- and space-resolved phonon detector. In addition to describing our own findings, we review a number of papers that we feel are pertinent to this goal.

The binding energies of FE's and BE's are on the scale of the binding energy of an electron to a shallow-donor impurity,

$$E_D = \frac{m^* e^4}{2\varepsilon_0^2 h^2} = \frac{13.6(m^*/m)}{\varepsilon_0^2} \text{ eV} , \quad (1)$$

where m^*/m is the effective-mass ratio for electrons and ε_0 is the static dielectric constant for the semiconductor. This Bohr model gives $E_D = 5.8$ meV for GaAs and a Bohr radius of 100 Å. The lattice spacing in GaAs is 5.7 Å, so the electron wave function extends over many lattice sites and the species of shallow-donor atom has little effect on the binding energy.[1] A similar calculation for shallow acceptors, using the effective-mass ratio for holes, gives a binding energy of 34 meV. Group-IV atoms can substitute for either Ga or As to become donors or acceptors, respectively. Group-IV atoms are common impurities, with Si often being a shallow donor and C a shallow acceptor.[2]

The method we use for detecting phonons by excitonic photoluminescence is illustrated in Fig. 1. A single-crystal substrate with an epitaxially grown layer of controlled purity is cooled to liquid-He (LHe) temperatures. A focused low-power laser beam (the "probe") excites electrons and holes in a small region of the epilayer. The electrons and holes quickly form excitons. The recombination luminescence is dispersed by a spectrometer and detected by photon counting. A high-power laser beam (the "pump") is focused onto a metal film on the opposite crystal surface. Phonons emitted by the metal film cross the substrate and interact with excitons in the epilayer. We observe decreases in certain lines of the photo-

0163-1829/94/49(23)/16427(14)/$06.00 ©1994 The American Physical Society

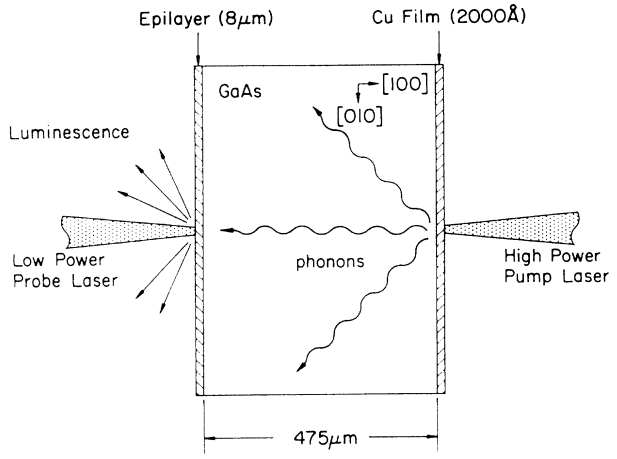

FIG. 1. Schematic of the experiment. The low-power probe laser creates electron-hole pairs which form excitons. The recombination luminescence is collected through a spectrometer and recorded by time-resolved photon counting. A high-power pump laser creates nonequilibrium phonons on the opposite crystal face which interact with the excitons in the epilayer. (Further experimental details are in Fig. 4 below.)

luminescence (PL) spectrum caused by nonequilibrium phonons (NEP's). Other researchers have employed optical means for detecting nonequilibrium acoustic phonons at low temperatures, as referenced later in the paper, but our method is distinguished, we believe, by its space and time resolution.

Our experiments relate to both the fields of phonon physics and the physics of shallow impurities in epilayers. The thermodynamics of excitons in a semiconductor, including interactions with impurities, dislocations, surfaces, and phonons, is an area of great interest. A phonon detector using impurity-bound excitons to detect NEP's with high spatial and temporal resolution has practical applications in phonon-imaging experiments. The focused laser beams can be easily moved on the sample surfaces to select phonon propagation direction. Also, the lasers can be pulsed to select phonon time of flight. Finally, since the spectrometer separates the PL of BE's with different binding energies, the induced changes in their relative populations (detected by the intensity of spectral lines) should depend on the frequency distribution of incident phonons.

The probe laser can be scanned spatially to detect the phonon flux at any point on the epilayer for phonon-imaging experiments. This is in contrast to typical phonon-imaging experiments which use a small superconducting device as the phonon detector, so the phonon source (laser or e beam) must be scanned to obtain an image. It is desirable in some cases to have a scannable detector, for example, when one wants to study the phonons emitted by a fixed source or to generate phonons of known frequency distribution. Scannable detectors have been used for studying the emission of phonons from electrical devices, as previously shown by Challis, Kent, and Rampton[3] and reviewed by Dietsche.[4] Additional applications may also include the imaging of structures within crystals (acoustic tomography) as demonstrated by Huebener and co-workers,[5–7] who used several fixed detectors. Other types of phonon detectors using optical methods have been demonstrated.[8] Often they involve the introduction of impurities into the sample or are suited to a specific crystal material.

II. PHOTOLUMINESCENCE SPECTRUM OF GaAs

Figure 2 shows a PL spectrum at 1.62 K for the undoped, slightly p-type GaAs sample we studied. The details concerning the measurement of this spectrum are covered in Sec. VI. The peaks are identified from their wavelengths and shapes. We are mainly concerned with the free excitons and shallow impurity-bound excitons which occur at higher photon energy (short wavelength). Figure 3 shows an expansion of this part of the spectrum.

Several papers[9–14] give energies associated with the excitonic transitions or show PL spectra from which the energies can be measured. The published wavelengths corresponding to specific features often vary by a few angstroms, perhaps due to variances in spectral calibrations or shifts due to crystal stress induced by sample mountings.[11] Our analysis is consistent with energies published by Williams and Bebb[13] (abbreviations defined below):

Species	Energy	Wavelength
FE	1.5156 eV	8182 Å
(D^0,X)	1.5145 eV	8188 Å
(D^+,X)	1.5133 eV	8194 Å
(A^0,X)	1.5125 eV	8198 Å

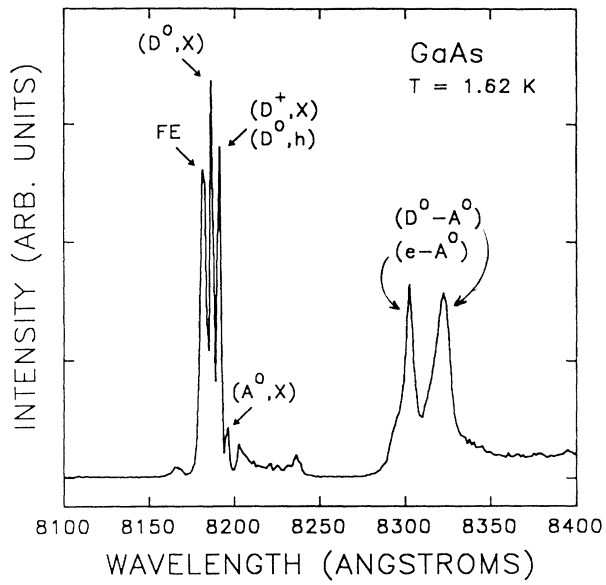

FIG. 2. Photoluminescence spectrum of epitaxial GaAs at 1.62 K. The lines are labeled as FE, free-exciton recombination; (D^0,X), shallow neutral donor bound-exciton recombination; (D^+,X), shallow ionized donor bound-exciton recombination; (D^0,h), shallow neutral donor free-hole recombination; (A^0,X) shallow neutral acceptor bound-exciton recombination; $(D^0$-$A^0)$, donor-to-acceptor pair transition; and $(e$-$A^0)$, conduction-band-to-acceptor transition.

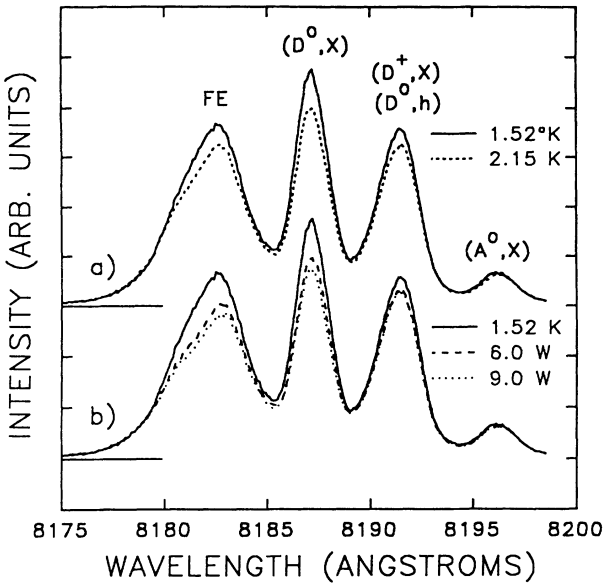

FIG. 3. (a) Comparison of excitonic intensities at 1.52 K (solid line) and 2.15 K (dashed line). (b) Comparison of excitonic intensities with no pump laser (solid line), pump laser with 6.0 W peak power (dashed line), and pump laser with 9.0-W peak power (dotted line). See Sec. VI for further experimental conditions.

Comparison of these energies to our data leads to the following identification of our experimental lines. The shortest-wavelength peak ($\lambda=8183$ Å in Fig. 3) is from the radiative recombination of free excitons (labeled FE). The second peak ($\lambda=8187$ Å) is due to radiative recombination of excitons bound to neutral shallow donors (labeled D^0,X). The peak at 8192 Å corresponds to two processes: the recombination of excitons bound to ionized shallow donors (labeled D^+,X), and free holes recombining with neutral donors (labeled D^0,h). The latter two transitions occur at almost the same energy in GaAs and cannot be resolved separately here. The peak at 8196 Å is from the radiative recombination of excitons bound to neutral shallow acceptors (labeled A^0,X). The peaks around 8300 Å are from donor-to-acceptor pair (D^0-A^0) (an electron from a donor recombines with a hole on an acceptor) and conduction-band-to-acceptor (e-A^0) transitions.

The relative intensities of the spectral lines vary widely between samples. The intensity of any excitonic line depends on the number of excitons in that state, their energy distribution, and the transition probability for radiative recombination. All three factors are important. For example, our sample is p-type yet the (D^0,X) line is much more intense than the (A^0,X) line because the transition probability (oscillator strength) is much higher for (D^0,X) than for (A^0,X). There is also evidence that interaction between crystal defects affects the intensity ratios. It has been shown that the acceptorlike defect commonly labeled A causes a strong quenching of the (D^0,X) line so that its relative intensity in the spectrum is not proportional to the number of shallow donors in the sample.[15]

The intensity of the lines in the PL spectrum is affected by varying the sample temperature or by creating nonequilibrium phonons, as shown in Fig. 3 and described in Sec. VI. The reader may wish to read that section next. We now consider some of the physical processes involved in these effects.

III. KINETICS OF IMPURITY-BOUND EXCITONS

In an attempt to understand the changes in the PL spectra of Fig. 3, we first examine the kinetics of excitons in a semiconductor epilayer using the energy levels and time scales for GaAs. We imagine the steady-state case of uniform optical generation of electrons (e) and holes (h) which quickly (in subnanoseconds) form excitons. A constant volume of excitons is assumed (i.e., no diffusion or reabsorption of the PL of recombining excitons). We consider a low-temperature (1.8-K) regime and a single impurity species. We used a low excitation power density of the probe laser (~ 3 mW/cm^2); therefore, it is safe to assume that there are many more impurity sites than excitons, so saturation effects are negligible. The formalism we use is that used by Hwang[9] but our treatment has some significant differences to be discussed later. A review of the properties of BE's in semiconductors has been published by Dean and Herbert.[16]

In this ideal system we express the rate equations for the density of free and bound excitons as

$$\frac{dn}{dt}=G-\frac{n}{\tau_R}-\frac{n}{\tau_{\rm NR}}-nAN_B+Bn_B\ , \tag{2}$$

$$\frac{dn_B}{dt}=nAN_B-\frac{n_B}{\tau_{RB}}-\frac{n_B}{\tau_{\rm NR}B}-Bn_B\ , \tag{3}$$

where n is the density of free excitons and n_B is the density of BE's. τ_R is the FE radiative decay time, which is generally assumed to be longer than the characteristic times of other processes depleting FE's. FE's recombine nonradiatively, especially at surfaces and crystal defects, with a rate $1/\tau_{\rm NR}$ which varies with the quality of individual samples. B is the thermal detrapping rate for BE's returning to FE's and $\tau_{\rm RB}$ and $\tau_{\rm NR}B$ are the radiative and nonradiative decay times for BE's.

G is the generation rate of FE's from e-h pairs created by the probe laser. These carriers may recombine radiatively (although the recombination time is long compared to formation of FE's, etc.[9]), be captured by impurities,[17] recombine nonradiatively at defects and surfaces, or form FE's. The relative probabilities of these recombination mechanisms will be discussed in Sec. IV.

For a density of impurities N_B the trapping of FE's by impurities to form BE's occurs at the rate AN_B. A method for directly measuring the trapping time of FE's by impurities in CdS has been reported by Henry and Nassau.[18] The lifetime of a BE luminescence line is measured by the phase-shift technique for two slightly different excitation photon energies. The delay time of e-h pairs created by slightly below-band-gap photons that could form BE's but not FE's is compared to that of e-h pairs created by slightly above-band-gap photons which could form FE's which were then trapped to become

BE's. The difference in delay between the two cases corresponds to a trapping time of 0.65–1.3 ns for undoped crystals. The measured trapping time becomes negligible compared to the 1-ns radiative decay time for lightly doped samples. A similar measurement by Minami and Era[19] using a mode-locked dye laser and single-photon counting to achieve 100-ps time resolution found a trapping time of 0.9 ns for a high-purity CdSe sample. We are unaware of such an experiment reported for GaAs; however, the rise times of BE lines in PL experiments are subnanosecond,[14,20] implying that the time for FE's to be trapped or decay nonradiatively is also a subnanosecond process.

In addition to the equilibrium phonons present at the ambient temperatures, the PL measurement introduces additional phonons which can detrap the BE. Phonons are emitted by hot electrons excited with above-band-gap photons as they lose kinetic energy before combining to form excitons or being trapped by impurities.[17] Excitons recombining nonradiatively also emit phonons. To reduce the number of the latter nonequilibrium phonons, we use a lower-power He-Ne laser ($\lambda=6328$ Å) for the probe.

It is usually assumed that the effects of ambient thermal phonons detrapping BE's are negligible since the binding energy of a BE is much larger than $k_B T$ at LHe temperatures. For example,[21] in GaAs the shallow neutral donor BE, labeled (D^0,X), has a binding energy of 1.1 meV while $k_B T=0.138$ meV for 1.6 K. It is true that most of the ambient phonons do not have enough energy to detrap BE's, but the high-energy tail of the Planck distribution does cause an exponential temperature dependence in the number of phonons available to detrap BE's. Using the conversion 1 meV=242 GHz, a phonon must have $\nu \geq \nu_D = 266$ GHz to detrap the (D^0,X) BE. The number of phonons able to detrap this exciton is

$$N(\nu_D,T) \propto \int_{\nu_D}^{\infty} \frac{\nu^2}{e^{h\nu/kT}-1} d\nu \ , \tag{4}$$

assuming the low-frequency regime where the phonon density of states is given by

$$g(\nu) \propto \nu^2 \ . \tag{5}$$

For example, evaluating this result numerically one finds that, with $\nu_D = 266$ GHz,

$$\frac{N(\nu_D, 2.15\ \text{K})}{N(\nu_D, 1.52\ \text{K})} \simeq 18 \ , \tag{6}$$

so in an equilibrium situation there is a significant temperature dependence of the detrapping rate even at LHe temperatures, although the change in the total number of trapped excitons is considerably smaller. In addition, the short lifetime of excitons in GaAs precludes them coming into thermal equilibrium with the lattice. We will return to this point later.

The rate equation for the density of BE's, Eq. (3), is similar to that for FE's. The lifetime for BE decay was measured for shallow impurities in GaAs using the optical phase-shift technique in 1972 by Hwang and Dawson[21] who reported $\tau_{D^0}=1.07\pm0.1$ ns, $\tau_{D^+}=0.80\pm0.08$ ns, and $\tau_{A^0}=1.6\pm0.16$ ns, for excitons bound to neutral donors (D^0), ionized donors (D^+), and neutral acceptors (A^0), respectively. Finkman, Sturge, and Bhat[14] used a mode-locked dye laser to directly excite the (D^0,X) (avoiding the problem of trapping-time uncertainty) and a single-photon-counting detection system to give a time response of 0.35 ns. They found $\tau_{D^0}=0.75\pm0.15$ ns and $\tau_{A^0}=1.0\pm0.1$ ns as a lower limit on the BE radiative lifetimes (τ_{RB}). They report that the lifetime is significantly reduced if the samples are strained.

The measured lifetime of (D^0,X) is significantly longer than theoretical predictions. Rashba and Gurgenishvili[22] and Rashba[23] have predicted that, since the binding energy of a BE is relatively small, the volume of its wave function is large compared to that of a crystal unit cell and this would result in very short BE lifetimes, especially of (D^0,X) in GaAs. There have been corrections to their original quantitative estimates, but the theoretical values reported by Sanders and Chang[24] in 1983 of $\tau_{D^0}=0.031$ ns and $\tau_{A^0}=0.96$ ns for GaAs are typical. The (A^0,X) lifetime is comparable between experiment and theory, but the theoretical prediction for τ_{D^0} is more than 20 times shorter than the experimental measurement. Sanders and Chang[24] report similar discrepancies for other semiconductors. Finkman, Sturge, and Bhat[14] suggest that rotational degeneracy of the (D^0,X) may be responsible for its long lifetime, but we know of no detailed calculations confirming this.

What is the principal process by which BE's decay nonradiatively? The rate for cascade multiphonon emission (a BE recombining by giving all its energy to phonons) is thought to be small for shallow-impurity BE's in GaAs,[21] but may be important for deep impurities in GaAs and GaP,[25] or in special systems [e.g., Er^{3+} in LAF_3 (Refs. 26 and 27)]. Another mechanism for nonradiative decay of an exciton bound to a neutral donor is an Auger process in which an electron and hole recombine and eject an additional electron with high kinetic energy. This is thought to be the principal BE decay channel in several indirect-gap semiconductors. For example, in GaP the predicted radiative lifetime of (D^0,X) is 11 μs, but the measured decay time is 21 ns.[28] Similarly the predicted radiative lifetime of (D^0,X) in Si is 750 μs, whereas the observed 80-ns lifetime is attributed to Auger recombination.[28] It is generally assumed that the Auger recombination rate for (D^0,X) in most direct-gap semiconductors is much lower than the radiative recombination rate.[16,18,24,29,30] Support for this assumption in GaAs has been reported by Wolford and coworkers[20,31,32] who applied high pressure to GaAs at low temperatures until it became an indirect-gap semiconductor. At the transition, the lifetime of (D^0,X) increased from 1 to 20 ns, suggesting that radiative decay limits the (D^0,X) lifetime at zero stress.

IV. EFFECT OF EQUILIBRIUM PHONONS ON EXCITONS

The experiments we report below involve relatively long time scales (≥ 50 ns) compared to the total lifetimes

of BE's and FE's. Therefore n and n_B reach steady-state values ($dn/dt = dn_B/dt = 0$). There are several BE states in a real crystal, so we shall now distinguish between them by defining

$$n_B = \sum_i n_i \ , \tag{7}$$

with n_i the density of the ith BE species.

Equations (2) and (3) then become

$$\frac{dn}{dt} = 0 = G - \frac{n}{\tau_R} - \frac{n}{\tau_{\rm NR}} + \sum_i (Bn_i - nA_iN_i) \ , \tag{8}$$

$$\frac{dn_i}{dt} = 0 = nA_iN_i - \frac{n_i}{\tau_{Ri}} - \frac{n_i}{\tau_{{\rm NR}i}} - Bn_i \ . \tag{9}$$

Figure 3 shows that the intensity of the FE line decreases when the temperature is increased from 1.52 to 2.15 K. The measured intensity $I(T)$ of the FE is given by

$$I(T) \propto \frac{n}{\tau_R} \ , \tag{10}$$

where n is determined by solving Eqs. (8) and (9).

It is instructive to consider the temperature dependences of various terms in these equations. G is the generation of FE's from free carriers and should only vary if the relative probabilities of recombination by various processes vary. For example, Akimov *et al.*[33,34] see a quenching of the conduction-band–acceptor line (e-A^0) in GaAs as the temperature is raised, because thermally activated capture of electrons by nonradiative recombination centers depletes the free electrons. However, in our experiment we only see a rapid T dependence in the FE, (D^0,X), and (D^+,X) intensities; the lines around $\lambda = 8300$ Å do not change from 1.523 to 2.15 K. Recent experiments have shown that the number of free carriers available to form excitons is limited by nonradiative recombination near the surfaces, since very long carrier lifetimes are seen in "surface-free" structures where the carriers are confined by doping the surrounding regions.[35–39] Therefore we believe that G can be considered temperature independent in this small temperature range.

Because only a small number of the trapped excitons are detrapped by thermal phonons at $\simeq 2$ K, we ignore the contribution of thermally detrapped excitons (Bn_i) to n. The two states in which we observe PL reductions when increasing the liquid-He bath temperature show only a small absolute reduction, not all of which is due to detrapping. Therefore, these detrapped BE's will not contribute significantly to n. We also expect that the rate of trapping of FE's to form BE's by any species, A_iN_i, is temperature independent even though at higher temperatures thermal ionization of some states (e.g., neutral shallow donors become ionized donors) will reduce N_i. We know of no relevant thermally activated mechanism for FE's to recombine nonradiatively at these temperatures, so we expect that $\tau_{\rm NR}$ does not depend significantly on temperature.

From the above arguments we expect that the FE density n does not depend strongly on temperature unless the radiative recombination process becomes competitive with the nonradiative recombination. Smith *et al.*[36,37] etched the doping layer which was confining the FE in their GaAs homostructure and saw a large decrease in the recombination luminescence intensity, implying that surface recombination dominates in samples like ours. Most importantly, we see no change in the (A^0,X) line with temperature, so either the density of FE's available to be bound is constant or other terms in Eq. (9) change with temperature to exactly compensate for a change in n.

Considering Eq. (10), we thus conclude that the dominant cause for the observed reduction in the FE line with increasing temperature is an increase in the radiative lifetime with lattice temperature. The following simple calculation illustrates theoretically how the radiative lifetime of FE's is dependent on the kinetic-energy distribution of excitons and, therefore, upon the lattice temperature.

Momentum conservation requires that

$$k_{\rm photon} = k_{\rm FE} \tag{11}$$

for radiative recombination to occur. Now,

$$k_{\rm photon} = \frac{E_{\rm photon}}{\hbar c} \ , \tag{12}$$

where $E_{\rm photon}$ is the recombination photon energy (1.5156 eV). Assuming a parabolic energy dispersion for the FE, the kinetic energy of a FE satisfying Eq. (11) is

$$\Delta = \frac{\hbar^2 k_{\rm FE}^2}{2m^*} = \frac{E_{\rm photon}^2}{2m^* c^2} \ , \tag{13}$$

where m^* ($= m_e^* + m_h^* \simeq 0.5 m_0$) is the effective mass of the FE. We find

$$\Delta = 2.25 \times 10^{-6} \text{ eV} \tag{14}$$

is the kinetic energy of a FE which recombines radiatively.

For the simple case of isotropic masses, the density of FE's with energy E at temperature T is

$$n(E,T) = B(T) g(E) e^{-E/kT} \ , \tag{15}$$

where

$$g(E) = E^{1/2} \tag{16}$$

is proportional to the density of states and $B(T)$ is a normalization constant determined by

$$\int_0^\infty B(T) E^{1/2} e^{-E/kT} dE = n \ , \tag{17}$$

where n is the (assumed constant) density of FE's. Some algebra yields

$$B(T) = \frac{2n}{\sqrt{\pi}(kT)^{3/2}} \ , \tag{18}$$

so for two temperatures T_1 and T_2 the ratio of density of excitons with energy Δ is

$$\frac{n(\Delta,T_2)}{n(\Delta,T_1)}=\left[\frac{T_1}{T_2}\right]^{3/2}\exp\left[-\frac{\Delta}{k}\left[\frac{1}{T_2}-\frac{1}{T_1}\right]\right]. \quad (19)$$

As T increases from 1.52 to 2.15 K, we predict

$$\frac{I(2.15\text{ K})}{I(1.52\text{ K})}=\frac{\tau_R(1.52\text{ K})}{\tau_R(2.15\text{ K})}=\frac{n(\Delta,2.15\text{ K})}{n(\Delta,1.52\text{ K})}=0.597\ . \quad (20)$$

Note that in this temperature range, the exponent in Eq. (19) is nearly unity and the change in radiative rate comes principally from the prefactor

$$\left[\frac{1.52\text{ K}}{2.15\text{ K}}\right]^{3/2}=0.594\ . \quad (21)$$

So, in this temperature range,

$$I(T)\propto n/\tau_R(T)\propto T^{-3/2}\ , \quad (22)$$

We see that this simple model predicts a decrease of 40% in $I(T)$, but only an 11% change is observed in the experimental intensity (Fig. 3). We have neglected any broadening of the recombination line with increasing temperature which would increase the recombination rate at higher temperatures. However, the most likely reason for a small reduction is that the FE's do not actually have the same temperature as the lattice. Let us consider why.

The photoexcited carriers generated by the probe laser ($h\nu\simeq 1.96$ eV) quickly lose most of their excess energy by emitting LO phonons, then relax more slowly by emitting acoustic phonons. It is known[35,40–47] that this relaxation is slow for high excitation densities, often resulting in minimum carrier temperatures greater than 15 K even though the lattice is at LHe temperatures. However, for low excitation densities, the carriers relax much more quickly and may come close to the lattice temperature before recombining.[17] For our incident probe power of 3 mW/cm^2, the results of Ulbrich[48] suggest that the photoexcited carriers cool to about 6 K before recombining. Clearly the effects of lattice phonons are reduced, leading to a smaller intensity reduction than is predicted.

An increase in τ_R with increasing temperature at low probe powers has been reported by others[35–39] in epitaxial structures where surface recombination is small. Smith *et al.*[36,37] fit their data by assuming recombination is possible only for excitons with kinetic energy less than $\Delta=0.5$ meV, while a similar analysis by 't Hooft *et al.*[38,39] gives $\Delta=0.7$ meV. The data of 't Hooft *et al.*[38,39] show an increase of the FE lifetime of about 10% from 1.5 to 2.0 K, which corresponds well with the 11% intensity reduction we see from 1.52 to 2.15 K (although the magnitude of our reduction depends on the probe power as explained in Sec. VI). Feldmann *et al.*[35] compute $\Delta=0.5$ meV at $T=50$ K and see no increase in PL intensity with decreasing temperature, indicating that radiative recombination dominates the excitonic decay for their sample.

Next we consider the temperature dependence of the PL for a shallow-impurity BE. (The kinetic-energy effect derived above does not apply to bound excitons.) First we assume that the FE density is constant, as above. We also ignore exciton-exciton interactions by assuming the exciton density is low. Therefore we define

$$G_i=nA_iN_i \quad (23)$$

as the temperature-independent generation rate at which FE's are trapped on BE's of type i. We then have

$$\frac{dn_i}{dt}=G_i-n_i\left[\frac{1}{\tau_{Ri}}+\frac{1}{\tau_{\mathrm{NR}i}}+B\right]=0\ . \quad (24)$$

As discussed in the last paragraph of Sec. III, the nonradiative recombination rate ($1/\tau_{\mathrm{NR}i}$) can be neglected and we obtain

$$\frac{dn_i}{dt}=G_i-n_i\left[\frac{1}{\tau_{Ri}}+B\right]=0\ , \quad (25)$$

which yields

$$n_i=\frac{G_i}{\left[\frac{1}{\tau_{Ri}}+B\right]}\ . \quad (26)$$

At $T=0$ K, there are no phonons available to detrap BE's and

$$n_i(T=0)=G_i\tau_{Ri}\ . \quad (27)$$

All trapped excitons recombine radiatively with a rate

$$R_{i0}(T=0)\equiv G_i=\frac{n_i}{\tau_{Ri}}\ . \quad (28)$$

In reality, a number of mechanisms other than radiative recombination are possible for decay of the BE state (Auger recombination, detrapping of the BE, etc.). The recombination rate for any mechanism l at temperature T compared to the radiative recombination rate is

$$\frac{R_{il}(T)}{R_{i0}(T)}=C_le^{-\Delta E_l/kT}\ , \quad (29)$$

where ΔE_l is the activation energy for state l and C_l is a temperature-independent constant.[29,49,50] The assumptions that G_i is constant and $dn_i/dt=0$ imply that

$$\sum_l R_{il}(T)=G_i \quad (30)$$

does not change with temperature. Thus, the radiative recombination rate at any temperature is given by

$$\frac{R_{i0}(T)}{R_{i0}(O)}=\frac{1}{1+\sum_l C_le^{-\Delta E_l/kT}}\ . \quad (31)$$

Equation (31) predicts the temperature dependence of the PL intensity. Several authors have determined activation energies and relative probabilities of decay by various mechanisms by fitting experimental PL intensities as a function of temperature with Eq. (31). Bogardus and Bebb[51] report that the temperature dependence of the (D^+,X) PL line for GaAs is fitted well with a single thermally activated process with $\Delta E=7$ meV corre-

sponding to a final state of an ionized donor and a free electron-hole pair. However, two mechanisms with activation energies of 7 and 1 meV are required to fit the (D^0,X) line. Two decay mechanisms with different activation energies were also used by Bimberg, Sondergeld, and Grobe[52] to explain the temperature dependence of the (A^0,X) line for $2<T<20$ K. A recent analysis of the (A^0,X) and several defect lines as a function of temperature requires two mechanisms with different activation energies to fit the data, but the authors of this recent study[53] point out that the confidence level with respect to the actual values of the activation energies is quite poor because of the strong correlation between C_l and ΔE_l.

V. EFFECT OF NONEQUILIBRIUM PHONONS ON THE BOUND-EXCITON POPULATION

How do NEP's change the steady-state BE distribution determined by the above equations? First we shall determine the relevant energy scales. In GaAs, the binding energies of excitons to shallow impurities, determined from the spectroscopic line spacings,[13] are 1.1 meV (266 GHz) for (D^0,X), 2.3 meV (556 GHz) for (D^+,X), and 3.1 meV (750 GHz) for (A^0,X), where the number in parentheses corresponds to the minimum frequency $\nu_D=E/h$ required for a phonon to dissociate the exciton from the binding site. It is difficult to estimate the frequency distribution of phonons arriving at the epilayer; however phonon-imaging experiments with similar excitation parameters and sample thicknesses have shown the dominant phonons arriving are well below 600 GHz in GaAs,[54,55] InAs, and other semiconductors.[56]

Previous experiments have detected electrons liberated from shallow donors by NEP's. In 1969 Crandall[57] reported generating high-frequency phonons by donor impact ionization in an epitaxial GaAs layer and then detecting them by an increase in the bias current through an identical layer on the opposite side of a 500-μm-thick substrate. Similar experiments detecting changes in photoconductivity caused by phonons emitted by a superconducting tunnel junction have been used to measure the electron binding energy for shallow impurities in Si and Ge.[58–61] These experiments did not have the temporal or spatial resolution to distinguish between ballistic and scattered phonons.

The energy required to ionize (remove an electron from) a shallow donor in GaAs is around 5.9 meV (depending on impurity concentration[62]), corresponding to $\nu=1430$ GHz, and the energy to ionize a shallow acceptor is much higher. These energies are much higher than the 1–3 meV required to detrap a BE from these impurities. Isotope scattering in these samples increases as ν^4, so we expect a scattering rate at least 600 times higher for 1500-GHz phonons than for 300-GHz phonons. Therefore it is highly unlikely that an impurity in our GaAs epilayer is ionized by a ballistic phonon. [An exception is the (D^+,X) which only requires 0.2 meV for $(D^+,X)\rightarrow D^0+h$.]

Another possibility is that NEP's will induce Auger nonradiative recombination of BE's. Gel'mont *et al.*[63] point out that in the ground state Auger recombination of BE's is suppressed by angular momentum conservation, but the Auger recombination probability is several orders of magnitude higher for BE's bound to excited states of the impurity corresponding to local vibrations of the center of mass. Such an excitation in CdS requires 2.5-meV activation energy (600-GHz phonons). Phonons are created by exciting a metal film evaporated on one side of a 20-μm-thick CdS crystal at 1.3 K with a nitrogen laser and PL spectra are recorded from the opposite face with and without NEP's present. An attenuation of the (D^0,X) line is observed when NEP's are present, but the FE line remains constant, implying an induced nonradiative process.[64,65] This group also studied the temperature dependence of the intensity of the (D^0,X) line from 1.3 to 50 K and they find evidence for two processes with activation energies of 2.5 meV (vibrational motion of the impurity) and 7.7 meV (detrapping of the BE).

Blank *et al.*[66] have extended this method to GaAs, finding evidence for two processes with activation energies of 0.9 and 5.5 meV. With additional evidence from photoconductivity and NEP-induced changes in PL similar to those reported here, they conclude that the small activation energy corresponds to excitation of the BE into an excited state where nonradiative (Auger) recombination is allowed.

Gel'mont *et al.*[63] estimate a lifetime of 0.1 ns for the BE's bound to an excited impurity and explain why Auger recombination is important for NEP's when it is considered unimportant for equilibrium phonons: At low temperatures, the impurity is in its ground state, so Auger recombination is suppressed. At higher temperatures the BE is detrapped by thermal phonons. It is only in a narrow temperature range that there are enough thermal phonons available to excite the impurity without detrapping the BE. Thus NEP's offer an effective means to probe this process. The possibility of an Auger recombination rate in GaAs comparable to the (D^0,X) detrapping rate was raised by Bogardus and Bebb[51] in 1968.

Akimov *et al.*[67] reported a reduction in BE PL intensity in Si due to NEP's generated by an electrical heater. A corresponding increase in the FE line is observed (exciton lifetimes in this indirect-gap material are much longer than in GaAs), followed by a decrease in both lines which they attribute to a "phonon wind" pushing the excitons back to the crystal surface where they recombine nonradiatively. There is a strong dependence of the magnitude and even sign of this effect on the surface condition of the samples, the heater power, and the phonon propagation distance and direction. A 200-ns heater pulse is used and ballistic onsets of the attenuation of the exciton lines, followed by long (several microsecond) tails, are observed. They attribute the long tails to a slow release of phonons near the heater.

The same group also studied the (D^0,h) transition (free hole to neutral donor) in GaAs and saw a decrease in its PL intensity lasting about 5 μs following a 100-ns heat pulse from a metal-film heater.[68] They also studied at 1.8 K a sample consisting of 100 GaAs quantum wells 114 Å wide with 80-Å $Al_{0.3}Ga_{0.7}As$ barriers on a 400-μm-thick substrate with a 0.5-μm GaAs buffer layer.[33,34] Excitons are created by exciting the epilayer with a He-Ne laser

and phonons are created on the opposite crystal face with a 200-ns YAG:Nd laser (where YAG is yttrium aluminum garnet). A quenching of the conduction-band–acceptor luminescence line in both the quantum wells and buffer layer is observed. They estimate an effective layer temperature by comparing the amount of quenching to luminescence spectra at higher temperatures and find the effective temperature of the quantum wells is always higher than that of the buffer layer. Heating of the electron gas enhances the thermally activated process of electron capture by nonradiative recombination centers, depleting the number of free electrons available and reducing the conduction-band–acceptor luminescence intensity. Again the luminescence reduction lasts for several microseconds.

Thus there are at least three processes by which NEP's may deplete a certain species of shallow-impurity BE. Of these, detrapping of BE's is clearly more significant than ionization of the impurity, and the experiments of Blank *et al.*[66] strongly support the dominance of an induced Auger recombination process in epitaxially grown films of GaAs. For a fast transverse (FT), slow transverse (ST), or longitudinal (L) phonon of frequency ν and mode j to be absorbed by a BE of impurity species i and destroy the BE by process p, we can define a cross section

$$\sigma_p = \sigma_i(\nu, j) \ . \tag{32}$$

The number of BE's at temperature T with NEP flux $F(\nu, j)$ is then

$$n_i(T,F) = \frac{n_i(0,0)}{1 + \sum_l C_l e^{-\Delta E_l / kT} + \sum_p F\sigma_p} \ , \tag{33}$$

using Eq. (31) and again assuming that the number of detrapped excitons does not contribute significantly to the FE density. The experimental case comparing n_i at temperature T with and without NEP's gives

$$\frac{n_i(T,F)}{n_i(T,0)} = \frac{1 + \sum_l C_l e^{-\Delta E_l / kT}}{1 + \sum_l C_l e^{-\Delta E_l / kT} + \sum_p F\sigma_p} \ . \tag{34}$$

The simplest case would be for $T=0$ K for a crystal with no scattering and only one BE depletion mechanism with activation energy ΔE_p. In the case where nonequilibrium phonons heat a point in the detecting film to temperature T^*, we have

$$n_i(F) = \frac{n_i(0)}{1 + Ce^{-\Delta E_p / kT^*}} \ , \tag{35}$$

where C contains the geometrical factors due to phonon focusing and the probability of an incident phonon being absorbed by the BE. Equation (31) was derived for the steady-state condition $dn_i/dt = 0$. In our experiments the heat pulses are at least 15 ns long, which is longer than the BE decay time, so it is proper to treat the BE density as a steady-state problem even though the phonon flux is varying on a longer time scale.

VI. EXPERIMENTS ON EPITAXIAL GaAs

A diagram of our experimental configuration appears in Fig. 4. The phonon pump is a cavity-dumped Ar^+ laser (all lines, $\lambda \simeq 5000$ Å) which is focused to a 10-μm spot by lenses L_1 and L_2. A computer can scan the spot horizontally or vertically by applying a control current to rotate the galvanometer-mounted mirrors (G_1). The spot size and scan range are measured by scanning it across a "laser target" of 20-μm-wide metal film lines evaporated on a thin glass slide and detecting the transmitted light as a function of spot position with a photocell. The probe is a He-Ne laser beam ($\lambda = 6328$ Å) pulsed by an acousto-optic modulator (AO) and focused by lenses L_3 and L_4. The probe beam is deflected down the PL collection path by a Melles Griot "cold mirror" (M_1) which reflects visible light but passes the infrared PL. The PL is collected by L_4 and focused onto the entrance slit of a SPEX 0.5-m Czerny-Turner spectrometer. A second set of galvanometer-mounted mirrors (G_2) scans both the focused probe and spectrometer collection spots. The PL is detected with an RCA C31034 photomultiplier tube (PMT) cooled to -30 °C. Mirrors on the sample holder allow us to view the relative positions of pump and probe laser spots. The sample is immersed in liquid helium in a cryostat.

The sample is an undoped, slightly p-type 8-μm-thick epilayer grown by molecular-beam epitaxy (MBE) on a 475-μm-thick GaAs substrate. The substrate (pump) side was polished in a methanol-Br solution and then covered with a 2000-Å evaporated Cu film. The sample was mounted to the sample holder with small dabs of silver paint at the edges to avoid strain.

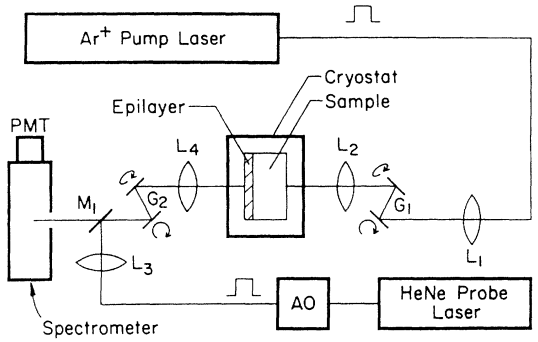

FIG. 4. Experimental configuration. The pulsed Ar^+ pump laser is focused onto the substrate crystal face by lenses L_1 and L_2. The focused spot can be scanned by moving the galvanometer mirrors G_1. The He-Ne probe laser is pulsed by the acousto-optic modulator (AO, synchronized to the pump pulse) and focused onto the epilayer by lenses L_3 and L_4. The focused probe spot is scanned by moving the galvanometer mirrors G_2. The luminescence is collected by L_4 and focused onto the entrance slit of the spectrometer. The photons are detected by a cooled photomultiplier tube (PMT). A "cold mirror" M_1 deflects the red probe beam but transmits the infrared luminescence.

Figure 3 shows the change in the steady-state PL spectrum for two temperatures and the effects of NEP's. The probe is at low power (3.75 μW power incident on the epilayer) and focused to a 200-μm spot ($\simeq 13$ mW/cm^2). This size was chosen to correspond to the bright "square" in the phonon-focusing pattern of (100) GaAs due to ST phonons.[69] It is essential to use low probe power densities to observe the effects discussed here because the probe also produces phonons which can detrap BE's. The effect of NEP's from the pump source on FE and BE luminescence is greatly reduced for higher probe powers. NEP's are created by pulses with a width of 15 ns from the cavity-dumped pump laser with a 500-kHz repetition rate. The group velocity of transverse phonons along [100] in GaAs is 3.35×10^5 cm/s, so the propagation time for ballistic phonons to cross our sample is 140 ns. To maximize the signal in Fig. 3 but still retain time-of-flight selection we use a 150-ns probe pulse beginning 130 ns after the pump-laser pulse.

The solid line in Figs. 3(a) and 3(b) is the PL spectrum at 1.52 K. The short-dashed line in (a) is obtained under the same conditions except the LHe bath temperature is adjusted to 2.15 K. For this small temperature change there is a significant reduction in the intensity of the FE (D^0,X) and (D^+,X) lines, but no appreciable change in the (A^0,X) line. Previously, strong temperature dependence of the BE PL intensity below 3 K was not observed by Bogardus and Bebb[51] or Bimberg, Sondergeld, and Grobe,[52] but a 10% decrease for (D^0,X) from 1.7 to 2.1 K was reported by Szafranek *et al.*[70] In our experiments, the magnitude of the reduction is greatly decreased when higher probe power densities are used.

Figure 3(b) shows PL spectra at 1.52 K but with NEP's created by the pump laser with peak incident powers of 6.0 W (long-dashed line) and 9.0 W (dotted line). The (D^0,X) line has the lowest exciton binding energy of the BE's and is reduced the most, as expected from the analysis in Sec. V. The percentage reduction of the (D^+,X) line is approximately the same for the 2.15-K steady-state and the 9.0-W spectra at 1.52 K. Finally, the (A^0,X) peak shows no detectable changes due to NEP's.

The time-dependent spectra taken at 1.6 K shown in Fig. 5 confirm the transient nature of this effect. The pump is a 15-ns-long 6.9-W pulse and the probe is a 65-ns, 9.8-μW pulse, centered at a delay time t_D after the center of the pump pulse. For each delay time a spectrum was taken with the pump (dashed line) and without the pump (solid line). At $t_D=0$ the effect of the pump is small, proving that cw heating due to the pump is negligible. For $t_D=100$ ns, the NEP's cause a slight reduction in the FE and (D^0,X) lines. The ballistic propagation time is 140 ns for transverse phonons, so this t_D samples the higher-velocity L phonons and the leading edge of the T-mode pulse, consistent with the nonzero width of the probe pulse. With $t_D=150$ ns, corresponding to the ballistic time of flight for T phonons, a large reduction of the FE and (D^0,X) lines and a slight reduction of the (D^+,X) line are observed. The reduction persists for a considerable time, as seen for $t_D=700$ ns.

We can directly observe the heat pulse by recording the PL intensity as a function of delay time for a fixed wavelength (a "time trace"). We reduce the probe pulse width to 50 ns and use 3.75-μW probe power. To increase the signal-to-noise ratio, we open the spectrometer slits from 100 to 200 μm. This 4-Å resolution gives the broader yet still distinguishable lines as shown in Fig. 6, but about four times higher photon count rate. We electronically scan the probe delay time at a rate of 9.3 ns per second.

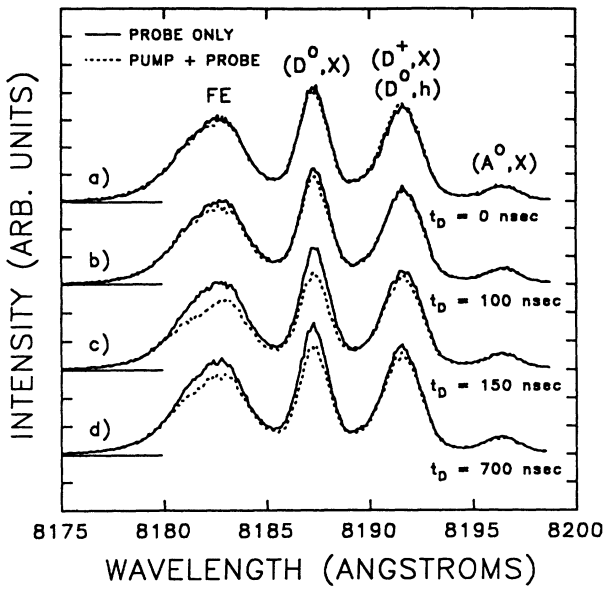

FIG. 5. Time-resolved spectra showing the NEP-induced changes in the luminescence created by the probe. Nonequilibrium phonons are generated on the substrate crystal face by a 6.9-W pump pulse. The time delay between the centers of the 65-ns probe and 15-ns pump pulses is t_D. The ballistic time of flight for T-mode phonons is 140 ns. Spectral resolution=2 Å.

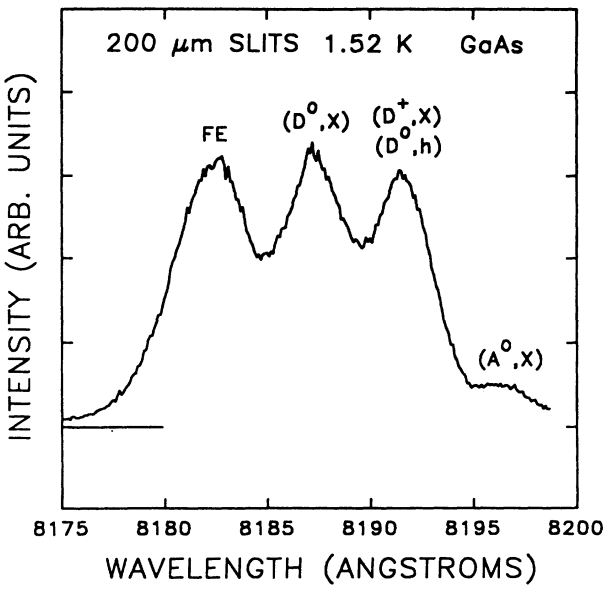

FIG. 6. Spectrum with 4-Å resolution used for recording time traces and images.

Figure 7 shows time traces for the FE line ($\lambda=8182$ Å) for several pump powers. The intensity falls sharply from its initial value I_0 to a minimum slightly after the ballistic-phonon arrival time, then rises slowly. This sharp onset demonstrates the ability of this method to time-resolve ballistic heat pulses. The reason for the slow recovery, observed also for the (D^0,X) and (D^+,X) lines, is not immediately apparent. The phonon source may have an extended lifetime due to the formation of a phonon "hot spot."[67–69,71–74] Alternatively, recent measurements on Si immersed in a He bath show that the cooling time of the heater film can be lengthened by the formation of a helium gas bubble at the excitation point.[75] Finally, the long tail could be associated with a quasidiffusive transport of phonons in the crystal. We also defocused the pump laser from a 10-μm-diameter to a 75-μm-diameter spot (corresponding to a decrease of 60 in power density) but saw the same time dependence. We have observed similar effects in MBE and metal-organic chemical-vapor-deposited (MOCVD) samples from several sources.

The pump power varies by a factor of about 2 between each trace in Fig. 7, yet the magnitude of the reduction is clearly not linear in pump power. Let us attempt to predict how the signal intensity of the FE scales with incident power, within the context of the discussion in Sec. IV. Equation (22) predicts the temperature dependence of the FE luminescence in a direct-gap semiconductor ideally scales as $T^{-3/2}$. Assume that the temperature of the crystal without NEP's is T_0. If a fraction f of the incident optical power P goes into a subset of NEP's which locally heat the epilayer, then the Stefan-Boltzmann law for phonons predicts (with NEP's) an epilayer temperature T given by

$$\sigma T^4=\sigma T_0^4+fP\ , \tag{36}$$

yielding

$$T=T_0(1+\kappa P)^{1/4}\ , \tag{37}$$

with $\kappa\equiv f/\sigma T_0^4$. Thus, with NEP's we expect the luminescence intensity to change by the ratio

$$I/I_0=(T/T_0)^{-3/2}=(1+\kappa P)^{-3/8}\ . \tag{38}$$

The fractional change in the luminescence intensity is given by

$$\Delta I/I\equiv(I_0-I)/I_0=1-(1+\kappa P)^{-3/8}\ . \tag{39}$$

At low powers ($\kappa P\ll 1$),

$$\Delta I/I\approx\tfrac{3}{8}\kappa P\ , \tag{40}$$

so the signal ΔI is nearly linear in P. At high powers, $\Delta I/I$ saturates at 1 (intensity completely quenched).

A comparison of this simplistic theory with experiment is shown in Fig. 8. The solid curve is a plot of Eq. (39) with κ adjusted to agree with the low-power data. The experimental data (the dots) are taken from the peak reductions in Fig. 7. We see that the signal rises approximately linearly with P at low powers, as predicted, and that there is a saturation in signal at high powers.

The saturation of the NEP signal is more pronounced in the experiments than in the simple theory. Two obvious factors are not accounted for in the theory: (1) the measured temperature dependence $I(T)$ is slower than $T^{-3/2}$, indicating an incomplete thermalization of the free excitons, and (2) NEP's are also produced by the probe beam. The second effect is demonstrated in Fig. 9, which shows the height of the FE line for a 200-ns probe starting 150 ns after the 15-ns pump pulse. In this experiment both pump and probe were focused to an $\sim$10-μm

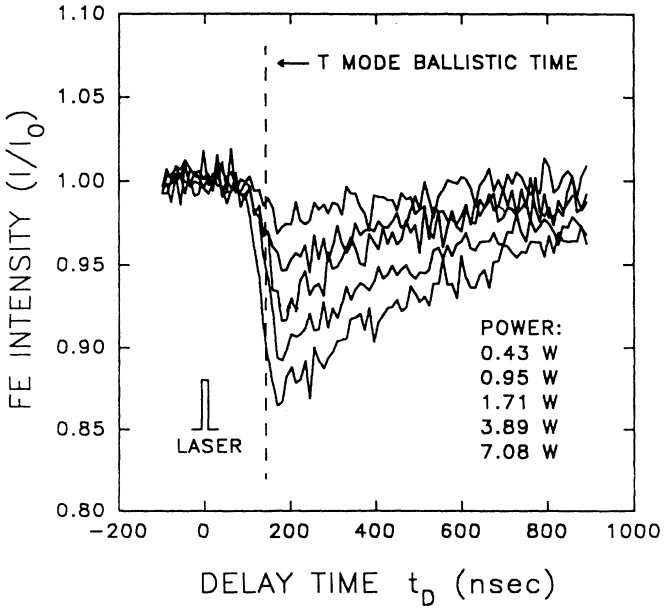

FIG. 7. Heat pulses detected by changes in the FE intensity I for several pump powers. I_0 is the FE intensity with no pump.

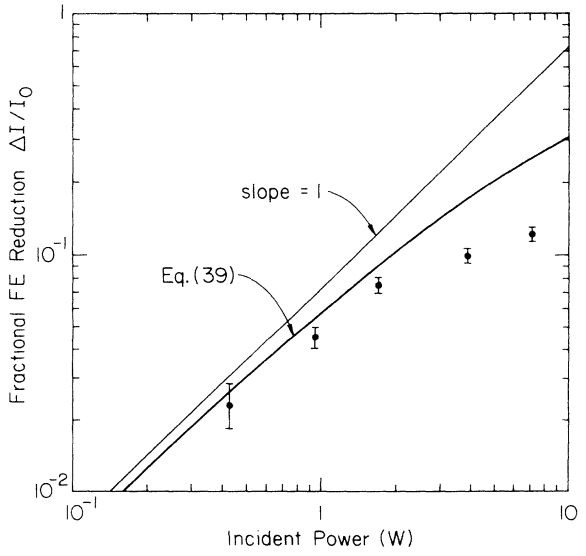

FIG. 8. Reduction of the FE line as a function of pump power, from the data in Fig. 7, compared to the simple theory described in the text.

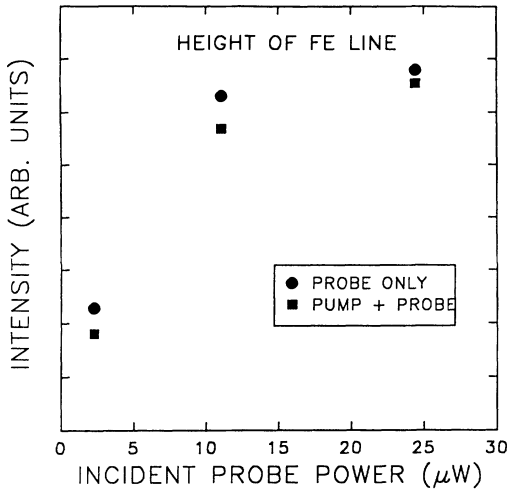

FIG. 9. Sublinear increase of the FE line intensity at high probe power densities and its reduction due to nonequilibrium phonons.

spot. The resultant probe power densities were relatively high ($\sim$3–30 W/cm^2), causing a sublinear increase of the FE peak height with the incident probe power due to the probe-generated NEP's. In fact the qualitative dependence on incident power is similar in both Figs. 8 and 9, although in each case the NEP flux is of a different origin. An analogous effect has been reported by 't Hooft, van der Poel, and Molenkamp[38] along with a linear dependence of PL intensity for lower probe power densities.

In Fig. 9, the percentage reduction due to NEP's created by the 6.0-W pump is highest for the 2.3-μW probe power, but the absolute difference is greatest for the 11-μW case. It is desirable to reduce the probe power to avoid these effects, but the reduction in signal-to-noise ratio at low count rates makes the experiments more difficult. An alternative approach is to use near-band-gap or even a resonant excitation, thus avoiding kinetic heating of the electron-exciton gas.

This analysis shows that a phonon detector based on bolometric (thermal) changes in FE luminescence is not likely to be a sensitive detector of NEP's. In particular, the FE signal is far less sensitive to T than a metal film biased at its superconducting transition, which undergoes a large fractional change in resistivity over 0.1 K or so. We have not attempted a quantitative analysis of the effect of NEP's on the BE luminescence, as the theory [e.g., Eq. (35)] contains several unknown parameters.

VII. PHONON IMAGING

A characteristic feature of ballistic phonons is phonon focusing, in which the flux emitted from a point source is concentrated along particular propagation directions.[66] To achieve sufficient angular resolution (see Fig. 1), we focus both pump and probe beams to 10 μm and scan the probe spot (which simultaneously scans the spectrometer collection spot) relative to the stationary pump beam. A tightly focused probe beam greatly increases the power density, so we expect to see less signal for an equivalent NEP flux, as explained above.

To form a 128×128 pixel image of phonon flux, we must record the PL intensity reduction for 16 000 detector positions. The entrance slit of the spectrometer is chosen to be 100 μm for good spatial resolution and a rear slit of 800 μm is selected to increase the count rate. For each probe position we record the number of FE luminescence photons during the heat pulse and subtract the number of FE photons detected 1400 ns after the pump pulse, using a 60-ns probe pulse. We integrate for 0.7 s per point and obtain the image shown in Fig. 10(a). A bright "square" is observed along [100] corresponding to the known phonon focusing of slow transverse (ST) phonons. For comparison we show in Fig. 10(b) a phonon image of (100) GaAs taken by biasing a superconducting tunnel junction into its bolometric-detection region. The signals from the superconducting detector are stronger and clearly show the characteristic caustic lines.

A better signal-to-noise ratio is obtained by scanning the probe beam slowly across the center of the square focusing structure. Figure 11 shows a comparison of line scans in the (010) plane, through the center of Fig. 10, for optical and electrical detection. The width and general

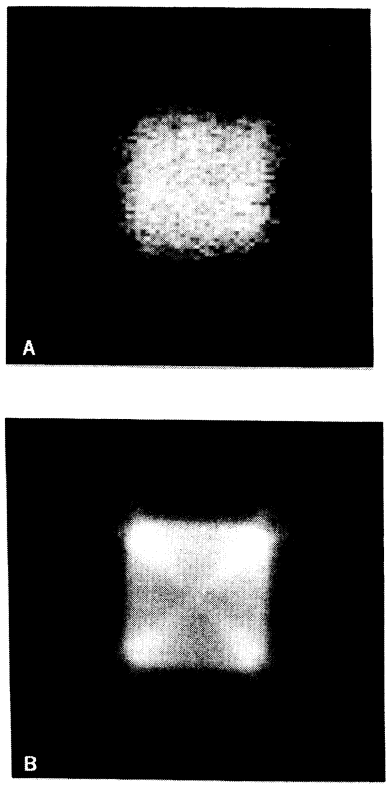

FIG. 10. Phonon images recorded from (a) NEP-induced changes in the FE line (probe scanned, pump fixed), and (b) current through a superconducting bolometer (pump scanned, probe fixed).

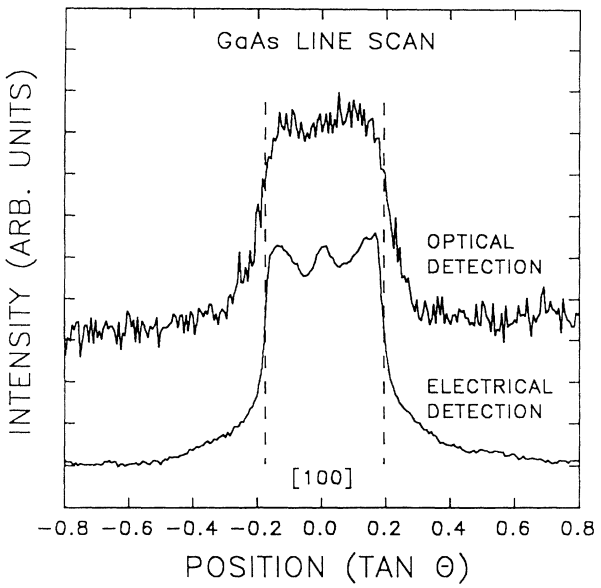

FIG. 11. Comparison of line scans in the (010) plane for optical and electrical (superconducting bolometer) detection. The dashed lines indicate the size of the phonon-focusing structure due to ST ballistic phonons (Ref. 69).

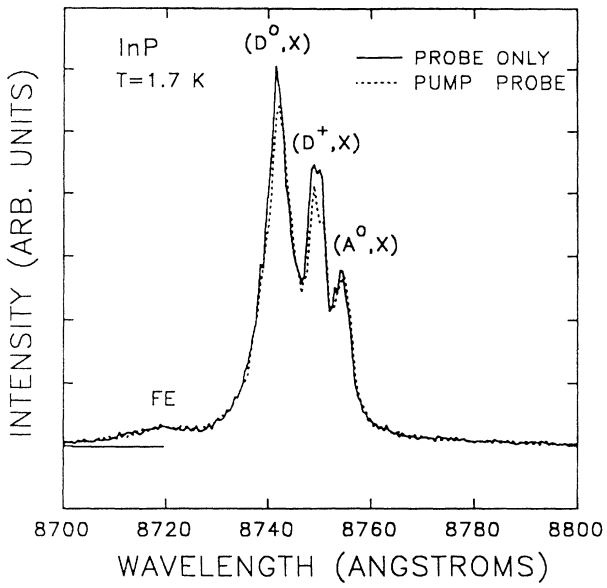

FIG. 12. Spectrum of InP at 1.7 K showing a reduction in the intensity of the donor bound-exciton lines caused by phonons created by the pump laser.

shape of the structures are the same, confirming that this experiment is detecting the focusing of ST phonons.

VIII. SUMMARY AND PROSPECTS

Our experiments show that the photoluminescence intensity of FE's and BE's in GaAs is sufficiently affected by NEP's to permit time-of-flight and imaging experiments of ballistic heat pulses. We have demonstrated an experimental configuration in which a probe beam and luminescence collection are simultaneously scanned in space. The temporal and spatial resolutions, in principle, are very high by virtue of photon counting and focused laser beams; however, at present, a full exploitation of these factors is limited by the relatively poor sensitivity compared to superconducting-film detectors.

A plausible explanation of the NEP-induced reduction in BE photoluminescence has been previously put forward by Gel'mont *et al.*[63] (for CdS) and by Blank *et al.*[66] (for GaAs). Basically, a nonequilibrium phonon excites the bound exciton into an excited state where nonradiative (Auger) recombination is possible. In this paper we have proposed a quite different mechanism for NEP-induced changes in the FE photoluminescence: in a direct-gap semiconductor, a local temperature rise at constant exciton density raises the FE kinetic energy and reduces the number of excitons that can radiatively decay. In fact, the populations of FE's and BE's are likely to be affected by a number of factors, and the kinetics of these and other excited states must be considered together in order to understand quantitatively both the temperature dependence and NEP sensitivity of various PL spectra.

We have preliminary results indicating that this technique is applicable to other semiconductor systems. Figure 12 is a PL spectrum of a 5-μm-thick InP epilayer grown on a 360-μm-thick InP substrate by MOCVD. This is a quasi-cw experiment where the pump is a cw Ar^+ laser modulated to give a 10-μs pulse every 100 μs. The (D^0,X) and (D^+,X) lines are noticeably attenuated by NEP's. (The lines were identified from the energy differences between them[10,11,76] although the whole spectrum is shifted by $\simeq 2$ meV from those previously published. This shift is possibly caused by a mounting-induced strain.[11]) We have also observed temperature- and NEP-induced changes in some parts of the PL spectrum of GaAs quantum wells.

ACKNOWLEDGMENTS

We thank S. Bose (Penn State University) for the GaAs sample used here and for providing us with a copy of his helpful thesis. We thank N. Pan (Raytheon), M. Razeghi (Thomson CSF), and H. Morkoç (University of Illinois) for other samples. We thank Y. C. Chang, M. Sturge, and D. Wolford for helpful discussions. We thank X. Zheng and J. Kim for help in the laboratory and interpreting results. This work is supported by the National Science Foundation under Materials Research Laboratory Grant No. DMR 89-20538.

*Present address: Advanced Micro Devices, Mail Stop 117, P.O. Box 3453, Sunnyvale, CA 94088-3453.

[1]G. E. Stillman, C. W. Wolfe, and J. O. Dimmock, in *Semiconductors and Semimetals,* edited by R. K. Willardson and A. C. Beer (Academic, New York, 1972), Vol. 12, p. 169.

[2]S. K. Ghandi, *VLSI Fabrication Principles* (Wiley, New York, 1983), p. 27.

[3]L. J. Challis, A. J. Kent, and V. W. Rampton, in *Phonons 89: Proceedings of the Third International Conference on Phonon Physics and the Sixth International Conference on Phonon Scattering in Condensed Matter, Heidelberg, 1989,* edited by S. Hunklinger *et al.* (World Scientific, Singapore, 1990), pp. 967,995.

[4]W. Dietsche, in *Phonon Scattering in Condensed Matter V,* edited by A. C. Anderson and J. P. Wolfe, Springer Series in Solid-State Sciences Vol. 68 (Springer-Verlag, Berlin, 1986), p. 366.

[5]R. P. Huebener, Rep. Prog. Phys. **47**, 175 (1984).

[6]W. Metzger, R. P. Huebener, R. J. Haug, and H. U. Habermeier, Appl. Phys. Lett. **47**, 1051 (1985).

[7]W. Klein, E. Held, and R. P. Huebener, Z. Phys. B **69**, 69 (1987).

[8]W. E. Bron, Rep. Prog. Phys. **43**, 301 (1980); K. Renk, in *Nonequilibrium Phonon Dynamics,* Vol. 124 of NATO Advanced Study Institute, Series B: Physics, edited by W. E. Bron (Plenum, New York, 1985), Chap. 2; W. P. Ambrose and W. E. Moerner, Phys. Rev. B **43**, 1743 (1991).

[9]C. J. Hwang, Phys. Rev. B **8**, 646 (1973).

[10]A. M. White, P. J. Dean, L. L. Taylor, R. C. Clarke, D. J. Ashen, and J. B. Mullin, J. Phys. C **5**, 1727 (1972).

[11]A. M. White, P. J. Dean, and B. Day, J. Phys. C **7**, 1400 (1974).

[12]U. Heim and P. Hiesinger, Phys. Status Solidi B **66**, 461 (1974).

[13]E. W. Williams and H. B. Bebb, in *Semiconductors and Semimetals,* edited by R. K. Willardson and A. C. Beer (Ref. 1), Vol. 8, p. 321.

[14]E. Finkman, M. D. Sturge, and R. Bhat, J. Lumin. **35**, 235 (1986).

[15]I. Szafranek, M. A. Plano, M. J. McCollum, S. L. Jackson, S. A. Stockman, K. Y. Chang, and G. E. Stillman, in *Impurities, Defects and Diffusion in Semiconductors: Bulk and Layered Structures,* edited by D. J. Wolford, J. Bernholc, and E. E. Haller, MRS Symposia Proceedings No. 163 (Materials Research Society, Pittsburgh, 1990), p. 193.

[16]P. J. Dean and D. C. Herbert, in *Excitons,* edited by K. Cho (Springer-Verlag, Berlin, 1979), p. 56.

[17]R. G. Ulbrich, Phys. Rev. Lett. **27**, 1512 (1971).

[18]C. H. Henry and K. Nassau, Phys. Rev. B **1**, 1628 (1970).

[19]F. Minami and K. Era, Solid State Commun. **53**, 187 (1985).

[20]H. Mariette, D. J. Wolford, and J. A. Bradley, Phys. Rev. B **33**, 8373 (1986).

[21]C. J. Hwang and L. R. Dawson, Solid State Commun. **10**, 443 (1972).

[22]E. I. Rashba and G. E. Gurgenishvili, Fiz. Tverd. Tela **4**, 1032 (1962) [Sov. Phys. Solid State **4**, 759 (1962)].

[23]E. I. Rashba, Sov. Phys. Semicond. **8**, 807 (1974).

[24]G. D. Sanders and Y. C. Chang, Phys. Rev. B **28**, 5887 (1983).

[25]C. H. Henry and D. V. Lang, Phys. Rev. B **15**, 989 (1977).

[26]A. Kiel, in *Quantum Electronics,* edited by P. Grivet and N. Bloembergen (Columbia University, New York, 1964), p. 765.

[27]M. H. Weber, Phys. Rev. **157**, 262 (1967).

[28]D. F. Nelson, J. D. Cuthbert, P. J. Dean, and D. G. Thomas, Phys. Rev. Lett. **17**, 1262 (1966).

[29]G. C. Osbourn and D. L. Smith, Phys. Rev. B **20**, 1556 (1979).

[30]W. Schmid and P. J. Dean, Phys. Status Solidi B **110**, 591 (1982).

[31]D. J. Wolford, in *Proceedings of the 18th International Conference on the Physics of Semiconductors,* edited by O. Engström (World Scientific, Singapore, 1987), p. 1115.

[32]D. J. Wolford and J. A. Bradley, Solid State Commun. **53**, 1069 (1985).

[33]A. V. Akimov, A. A. Kaplyanskii, V. I. Kozub, P. S. Kope'ev, and B. Ya Mel'tser, Fiz. Tverd. Tela **29**, 1843 (1987) [Sov. Phys. Solid State **29**, 1058 (1987)].

[34]A. V. Akimov, A. A. Kaplyanskii, V. I. Kozub, P. S. Kope'ev, and B. Ya Mel'tser, J. Lumin. **40&41**, 711 (1988).

[35]J. Feldmann, G. Peter, E. O. Göbel, P. Dawson, K. Moore, C. Foxon, and R. J. Elliot, Phys. Rev. Lett. **59**, 2337 (1987).

[36]L. M. Smith, D. J. Wolford, J. Martinsen, R. Venkatasubramanian, and S. K. Ghandi, J. Vac. Sci. Technol. B **8**, 8787 (1990).

[37]L. M. Smith, D. J. Wolford, R. Venkatasubramanian, and S. K. Ghandi, in *Impurities, Defects and Diffusion in Semiconductors: Bulk and Layered Structures* (Ref. 15), p. 95.

[38]G. W. 't Hooft, W. A. J. A. van der Poel, and L. W. Molenkamp, Phys. Rev. B **35**, 8281 (1987).

[39]G. W. 't Hooft, W. A. J. A. van der Poel, L. W. Molenkamp, and C. T. Foxon, *Excitons in Confined Systems,* edited by R. Del Sole *et al.* (Springer-Verlag, Berlin, 1988), p. 59.

[40]K. Kash, J. Shah, D. Block, A. C. Gossard, W. Wiegmann, Physica B+C **134B**, 189 (1985).

[41]J. Shah, Superlatt. Microstruct. **6**, 293 (1989).

[42]D. von der Linde and R. Lambrich, Phys. Rev. Lett. **42**, 1090 (1979).

[43]R. F. Leheny, J. Shah, R. L. Fork, C. V. Shank, and A. Migus, Solid State Commun. **31**, 809 (1979).

[44]K. Leo, W. W. Rühle, H. J. Queisser, and K. Ploog, Phys. Rev. B **37**, 7121 (1988).

[45]K. Leo, W. W. Rühle, and K. Ploog, Phys. Rev. B **38**, 1947 (1988).

[46]W. W. Rühle and H. J. Polland, Phys. Rev. B **36**, 1683 (1987).

[47]J. Shah and R. C. C. Leite, Phys. Rev. Lett. **22**, 1304 (1969).

[48]R. Ulbrich, Phys. Rev. B **8**, 5719 (1973); see also B. J. Skromme and G. E. Stillman, *ibid.* **29**, 1982 (1984).

[49]P. J. Dean, Phys. Rev. B **157**, 655 (1967).

[50]N. F. Mott, Proc. R. Soc. London, Sect. A **167**, 384 (1938).

[51]E. H. Bogardus and H. B. Bebb, Phys. Rev. **176**, 993 (1968).

[52]D. Bimberg, M. Sondergeld, and E. Grobe, Phys. Rev. B **4**, 3451 (1971).

[53]I. Szafranek, S. A. Stockman, M. Szafranek, M. J. McCollum, M. A. Plano, W. R. Miller, and G. E. Stillman, in *Degradation Mechanisms in III-V Compound Semiconductor Devices and Structures,* edited by V. Swaminathan, S. J. Pearton, and O. Manasreh, MRS Symposia Proceedings No. 184 (Materials Research Society, Pittsburgh, 1990), p. 109.

[54]S. E. Hebboul and J. P. Wolfe, J. Phys. B **74**, 35 (1989).

[55]G. A. Northrop, S. E. Hebboul, and J. P. Wolfe, Phys. Rev. Lett. **55**, 95 (1985).

[56]S. E. Hebboul and J. P. Wolfe, in *Proceedings of the 18th International Conference on the Physics of Semiconductors* (Ref. 31), p. 1377.

[57]R. S. Crandall, Solid State Commun. **7**, 1109 (1969).

[58]W. Burger and K. Lassmann, Phys. Rev. Lett. **53**, 2035 (1984).

[59]W. Burger and K. Lassmann, Phys. Rev. B **33**, 5868 (1986).

[60]K. Lassmann and W. Burger, in *Phonon Scattering in Condensed Matter V* (Ref. 4), p. 116.

[61]K. Lassmann, M. Gienger, and P. Gross, in *Phonons '89:*

Proceedings of the Third International Conference on Phonon Physics and the Sixth International Conference on Phonon Scattering in Condensed Matter, Heidelberg, 1989 (Ref. 3), p. 777.

[62]G. E. Stillmann, C. M. Wolfe, and J. O. Dimmock, in *Semiconductors and Semimetals* (Ref. 1), Vol. 12, p. 229.

[63]B. L. Gel'mont, N. N. Zinov'ev, D. I. Kovalev, V. A. Kharchenko, I. D. Yaroshetskii, and I. N. Yassievich, Zh. Eksp. Teor. Fiz. **94**, 322 (1988) [Sov. Phys. JETP **67**, 613 (1988)].

[64]V. C. I. Arakin, N. N. Zinov'ev, U. Parmanbekov, and I. K. Yaroshetskii, Solid State Commun. **55**, 733 (1985).

[65]N. N. Zinov'ev, D. I. Kovalev, and I. D. Yaroshetskii, Fiz. Tverd. Tela **28**, 3595 (1986) [Sov. Phys. Solid State **28**, 2026 (1986)]; N. N. Zinov'ev, D. I. Kovalev, V. I. Kozub, and I. D. Yaroshetskii, Zh. Eksp. Teor. Fiz. **92**, 1331 (1987) [Sov. Phys. JETP **65**, 746 (1987)].

[66]A. Yu. Blank, E. N. Zinov'ev, L. P. Ivanov, E. I. Kovalev, and I. D. Yaroshetskii, Fiz. Tehk. Poluprovodn. **25**, 67 (1991) [Sov. Phys. Semicond. **25**, 39 (1991)].

[67]A. V. Akimov, A. A. Kaplyanskii, E. S. Moskalenko, and R. A. Titov, Zh. Eksp. Teor. Fiz. **94**, 307 (1988) [Sov. Phys. JETP **67**, 2348 (1988)]; A. V. Akimov and A. A. Kaplyanskii, in *Phonons '89: Proceedings of the Third International Conference on Phonon Physics and The Sixth International Conference on Phonon Scattering in Condensed Matter, Heidelberg, 1989* (Ref. 3), p. 1242.

[68]A. V. Akimov, A. A. Kaplyanskii, V. V. Krivolapchuk, and E. S. Moskalenko, Pis'ma Zh. Eksp. Teor. Fiz. **46**, 35 (1987) [JETP Lett. **46**, 42 (1987)]; A. V. Akimov, A. A. Kaplyanskii, M. A. Pogarskii, and V. K. Tikhormirov, *ibid.* **43**, 259 (1986) [**43**, 333 (1986)].

[69]G. A. Northrop and J. P. Wolfe, in *Nonequilibrium Phonon Dynamics* (Ref. 8), Chap. 5.

[70]I. Szafranek, M. A. Plano, M. J. McCollum, S. A. Stockman, S. L. Jackson, K. Y. Cheng, and G. E. Stillman, J. Appl. Phys. **68**, 741 (1990).

[71]J. C. Hensel and R. C. Dynes, Phys. Rev. Lett. **39**, 969 (1977).

[72]J. A. Shields and J. P. Wolfe, Z. Phys. B **75**, 11 (1989).

[73]M. Greenstein, M. A. Tamor, and J. P. Wolfe, Phys. Rev. B **26**, 5604 (1982).

[74]Y. B. Levinson, in *Nonequilibrium Phonons in Nonmetallic Crystals,* edited by W. Eisenmenger and A. A. Kaplyanskii (North-Holland, Amsterdam, 1986), p. 91.

[75]J. A. Shields, M. E. Msall, M. S. Carroll, and J. P. Wolfe, Phys. Rev. B **47**, 12 510 (1993).

[76]W. Rühle and W. Klingenstein, Phys. Rev. B **18**, 7011 (1978).

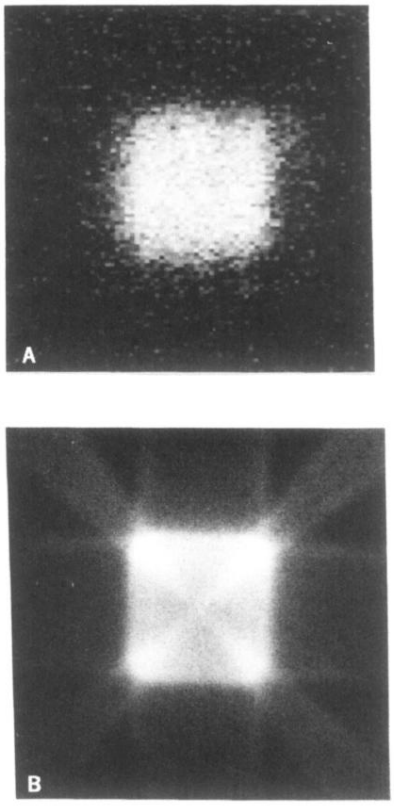

FIG. 10. Phonon images recorded from (a) NEP-induced changes in the FE line (probe scanned, pump fixed), and (b) current through a superconducting bolometer (pump scanned, probe fixed).